A Symbol-by-Symbol Channel Estimation Receiver for Space-Time Block Coded Systems and its Performance Analysis on the Nonselective Rayleigh Fading Channel

Cheng Shan, *Member, IEEE,* Pooi Yuen Kam, *Senior Member, IEEE,* and Arumugam Nallanathan, *Senior Member, IEEE*

***Abstract*—We present a symbol-by-symbol channel estimation receiver for an orthogonal space-time block coded system, and derive its analytical performance on a slow, nonselective, Rayleigh fading channel. Exact, closed-form expressions for its bit error probability (BEP) performance for M-ary phase shift-keying modulations are obtained, which enable us to theoretically predict the actual performance achievable under practical conditions with channel estimation error. Our BEP expressions show explicitly the dependence of BEP on the mean square error of the channel estimates, which in turn depend on the channel fading model and the channel estimator used. Tight upper bounds are presented that show more clearly the dependence of the BEP on various system parameters. Simulation results using various fading models are obtained to demonstrate the validity of the analysis.**

***Index Terms*—Space-time block codes, channel estimation, symbol detection, bit error probability, nonselective Rayleigh fading, Kalman filter, Wiener filter, PSAM.**

I. Introduction

TRANSMIT diversity coupled with the use of space-time coding is an effective technique to improve the performance of wireless systems [1]–[5]. In particular, space-time block codes (STBC) [4], [5] have been shown to have a simple decoder structure. A STBC with two transmit antennas was first introduced in [4], and it was later generalized for an arbitrary number of transmit antennas in [5]. The designs of orthogonal STBC were extensively studied and complex orthogonal designs (COD) were presented in [6]–[10] for more than two transmit antennas. The achievable rate of STBC is conjectured in [11]. A systematic construction of COD's achieving the rate bound proposed in [11] is presented in [12]. The designs in [12] are not given in closed-form linear combination format. Independently in [14], a systematic COD algorithm given in closed-form linear combinations of modulated symbols to reach the rate bound in [11].

Paper approved by R. W. Heath, Jr., the Editor for MIMO Techniques of the IEEE Communications Society. Manuscript received June 14, 2005; revised June 26, 2006 and April 12, 2007. This paper has been presented in part at the IEEE Globecom 2004, 29 Nov to 3 Dec 2004, Dallas, Texas, USA.

C. Shan is with the Global Standard Research Team, Samsung Electronics Co. LTD., Suwon, South Korea, 443-742 (e-mail: cheng.shan@samsung.com).

P. Y. Kam is with the Department of Electronics and Computer Engineering, National University of Singapore (e-mail: elekampy@nus.edu.sg).

A. Nallanathan is with Division of Engineering, King's College London (e-mail: arumugam.nallanathan@kcl.ac.uk).

Digital Object Identifier 10.1109/TCOMM.2008.1178

The beauty of STBC is that its orthogonal structure allows detection of individual symbols to be performed independently using only linear processing. This was shown in [4] for the case of perfect channel state information (CSI), i.e., when channel estimation is perfect. In practice, however, perfect channel estimates are not readily available, and one expects to perform simultaneous data detection and channel estimation. The aim of this paper is to develop a simple, symbol-by-symbol (SBS), channel estimation receiver for STBC. The work here can be considered as an extension of the work on optimum, SBS detection on nonselective Rayleigh fading channels for the case of a single transmit and multiple receive antennas [15]. Following the approach in [15], we arrive at a receiver structure which is similar to that in [4], with the actual channel fading gains replaced by their minimum mean square error (MMSE) estimates. We then obtain simple, exact, closed-form expressions as well as tight upper bounds for its bit error probability (BEP) performances with phase shift-keyed (PSK) modulations. The BEP results show clearly the dependence of BEP on the MSE of channel estimates, which in turn depends on the channel fading model, the additive channel noise level, and the estimator structure used. Finally the theoretical results are validated with simulations.

Performance results for STBC can be found in [16]–[23]. In [16]–[21], perfect CSI knowledge is assumed at the receiver. Specifically, in [16] exact BEP expressions of BPSK and QPSK for Alamouti's code [4] with one receive antenna is presented for both coherent and differential detection. In [17], error performance analysis is based on only those STBC's orthogonal in both space and time. In [18], the performance analysis is not general by taking a few STBC examples. The coherent results with PSK modulation under Rayleigh fading in [16]–[18] can be shown to be a special case of our work in this paper when there is no channel estimation error. In [19], the authors obtained a pair-wise error probability (PEP) expression based on perfect CSI knowledge using the moment generating function method, and the result is not in explicit form. Moreover, BEP is preferred over PEP for STBC systems. PEP is more suitable for space-time trellis codes. Symbol error probability expressions for M-PSK and M-QAM constellations over the keyhole Nakagami-m channel are presented in [20] assuming perfect CSI at the receiver. More recently in [21], an accurate BEP upper bound is proposed for a symbol-by-symbol detector for perfect CSI sceanario. Channel estimation error was taken into account in the PEP analysis approach in [22] while, however, computation of the eigenvalues of a correlation matrix is necessary. Reference [23] uses Alamouti's code [4] and pilot-symbol assisted modulation (PSAM) for channel estimation, but the BEP result is given in an unsolved integral form. In summary, the BEP results in [16]–[23] are either not explicit or assume perfect CSI at the receiver. Space-time trellis codes with first-order Markov channel model and Kalman filtering (KF) is proposed in [24]. In [25], a receiver for the Alamouti's STBC of [4] with two transmit and one receive antenna was proposed. This receiver is the same as our earlier receiver in [15]. It uses decision-directed KF for channel estimation, and considers a first-order Markov channel model. No BEP analysis is done, and BEP results are obtained only via simulations. Our present paper is more general than the work in the existing literature in that it builds on the theoretical foundation in [15] and presents exact, explicit, closed-form analytical BEP results.

Section II presents the system model, and introduces the SBS receiver. Section III derives the closed-form BEP expression for MPSK modulation with channel estimation, and Section IV shows how the BEP results are evaluated for various channel models and estimators. Simulation results in Section V confirm our analysis. A summary is given in Section VI.

II. System Model and Receiver Structure

A generalized complex orthogonal STBC for a multi-input-multi-output (MIMO) communication system with M_T transmit and N_R receive antennas is a $P \times M_T$ matrix $\boldsymbol{S}$. Each M_T-dimensional row vector of the code matrix $\boldsymbol{S}$ is transmitted through the M_T transmit antennas at one time, and the transmission of the matrix $\boldsymbol{S}$ is completed in P symbol periods. In this paper, we consider linear COD of STBC. During the P symbol periods, the system transmits$K$ symbols $s_k, k = 1, \ldots, K$, which are from a certain complex constellation. Each entry of $\boldsymbol{S}$ is a linear combination of $s_k, k = 1, \ldots, K$ and their conjugates s_k^*. The rate of the STBC is defined as K/P. In summary, a linear orthogonal STBC satisfies:

(i) Linearity: Each entry of $\boldsymbol{S}$ can be linearly decomposed as [6], [7]

$$\boldsymbol{S} = \sum_{k=1}^{K} (s_k \boldsymbol{A}_k + s_k^* \boldsymbol{B}_k) \tag{1}$$

where $\boldsymbol{A}_k, \boldsymbol{B}_k$ are $P \times M_T$ matrices with constant complex entries, e.g., the Alamouti code [4]:

$$\boldsymbol{S} = \begin{pmatrix} s_1 & s_2 \\ -s_2^* & s_1^* \end{pmatrix}, \text{ and}$$

$$\boldsymbol{A}_1 = \begin{pmatrix} 1 & 0 \\ 0 & 0 \end{pmatrix}, \boldsymbol{A}_2 = \begin{pmatrix} 0 & 1 \\ 0 & 0 \end{pmatrix},$$

$$\boldsymbol{B}_1 = \begin{pmatrix} 0 & 0 \\ 0 & 1 \end{pmatrix}, \boldsymbol{B}_2 = \begin{pmatrix} 0 & 0 \\ -1 & 0 \end{pmatrix}$$

(ii) Orthogonality: The matrix $\boldsymbol{S}$satisfies $\boldsymbol{S}^\dagger \boldsymbol{S} = \boldsymbol{D}$, where $\boldsymbol{S}^\dagger$ is the Hermitian transpose of $\boldsymbol{S}$, and $\boldsymbol{D}$ is a diagonal matrix [5]. Using the STBC property in (i), we have

$$\boldsymbol{S}^\dagger \boldsymbol{S} = \mathrm{diag}\left[\sum_{k=1}^{K} \lambda_{1,k}|s_k|^2, \ldots, \sum_{k=1}^{K} \lambda_{M_T,k}|s_k|^2\right] = \boldsymbol{D} \tag{2}$$

where $\{\lambda_{i,k}\}_{i=1}^{M_T}$ are non-negative numbers. For arbitrary signal constellations to satisfy the orthogonality condition in (2), one requires that

$$\begin{aligned} &\boldsymbol{A}_k^\dagger \boldsymbol{A}_k' + \boldsymbol{B}_k'^\dagger \boldsymbol{B}_k = \delta_{kk'} \mathrm{diag}[\lambda_{1,k}, \ldots, \lambda_{M_T,k}] \\ \text{and } &\boldsymbol{A}_k^\dagger \boldsymbol{B}_k' + \boldsymbol{A}_k'^\dagger \boldsymbol{B}_k = \boldsymbol{0} \end{aligned} \tag{3}$$

where $\delta_{kk'}$ is the Kronecker delta.

A. Transmitter

We assume M-PSK modulation and constrain the average transmitted energy per bit to a constant E_b. It is then easy to show that the total energy assigned to one block is $E_b K \log_2 M$. From the STBC definition in (2), it is clear that the total transmitted energy in a block is $\sum_{i=1}^{M_T} \sum_{k=1}^{K} \lambda_{i,k}|s_k|^2$. Thus, for each PSK symbol, the allocated energy is

$$E_s = |s_k|^2 = E_b K \log_2 M / \sum_{i=1}^{M_T} \sum_{k=1}^{K} \lambda_{i,k} \tag{4}$$

The symbol is now defined as $s_k = \sqrt{E_s} e^{j\phi_k}$, where ϕ_k takes on a value in the set $\{2n\pi/M\}_{n=0}^{M-1}$.

B. Receiver

Denoting the m-th transmitted signal block as $\boldsymbol{S}(m)$, the received signal matrix is

$$\boldsymbol{R}(m) = \boldsymbol{S}(m)\boldsymbol{H}(m) + \boldsymbol{N}(m) \tag{5}$$

Here $\boldsymbol{R}(m)$ is the $P \times N_R$ received matrix, where each entry $r_{pl}(m)$ is the received signal at the p-th symbol slot on the l-th receive antenna. $\boldsymbol{H}(m)$ is a $M_T \times N_R$ channel matrix, where each entry $h_{il}(m)$ is the fading gain on the il-th link, which is from the i-th transmit to l-th receive antenna, during the m-th block interval. The $h_{il}(m)$'s are spatially independent, identically distributed (i.i.d.), complex, Guassian processes from link to link. It is assumed in (5) that all the channels are block-wise constant, i.e., they remain constant for P symbol durations. All the theoretical derivations are based on this assumption in this paper unless otherwise stated. Thus, for each link, $\{h_{il}(m)\}_{m=0}^{\infty}$ forms a zero-mean, complex, Gaussian process with autocorrelation function $\mathrm{E}[h_{il}(m)h_{il}^*(m')] = 2\Omega(m-m')$. The system model is shown in Fig. 1. $\boldsymbol{N}(m)$ is the $P \times N_R$ noise matrix, whose entries $n_{pl}(m)$'s are i.i.d., zero-mean, complex, Gaussian random variables (r.v.'s) due to channel additive, white, Gaussian noise (AWGN) at the p-th symbol slot on the l-th receive antenna with $\mathrm{E}[n_{p'l'}^*(m')n_{pl}(m)] = \delta_{pp'}\delta_{ll'}\delta_{mm'}N_0$.

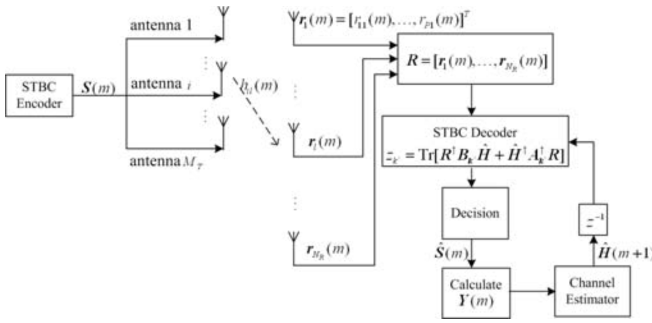

Fig. 1. System model and symbol-by-symbol channel estimation receiver structure.

C. Channel Estimation

We consider the decision feedback (DF) and the PSAM schemes for channel estimation here.

For DF scheme [15], [27], define the m-th decoded signal block as $\hat{\boldsymbol{S}}(m)$, and assume the signal-to-noise ratio (SNR) is sufficiently high so that all the past decisions can be assumed correct. The receiver performs modulation wipe-off on the past received blocks, and generates:

$$\begin{aligned}\boldsymbol{Y}(m') &= [\hat{\boldsymbol{S}}^\dagger(m')\hat{\boldsymbol{S}}(m')]^{-1}\hat{\boldsymbol{S}}^\dagger(m')\boldsymbol{R}(m') \\ &= v\boldsymbol{H}(m') + \tilde{\boldsymbol{N}}(m'),\ 0 \le m' \le m-1\end{aligned} \tag{6}$$

$\boldsymbol{Y}(m')$ is a noisy observation on the channel matrix $\boldsymbol{H}(m')$, and each entry $y_{il}(m'), i = 1 \ldots M_T, l = 1 \ldots N_R$ of $\boldsymbol{Y}(m')$ can be expressed in the form $y_{il}(m') = h_{il}(m') + \tilde{n}_{il}(m')$, where $\{\tilde{n}_{il}(m')\}_{m'}$ is a set of i.i.d., zero mean, complex, Gaussian r.v.'s with variance $[\sum_{k=1}^{K} \lambda_{i,k}]^{-1} E_s^{-1} N_0$. Define $\Lambda(m) = \{\boldsymbol{Y}(m'),\ 0 \le m' \le m-1\}$ as the information set containing the channel measurements available to the receiver up to the beginning of the m-th block.

After decoding the current block $\boldsymbol{S}(m)$, the measurement $\boldsymbol{Y}(m)$ is obtained and fed back to update the channel estimator. A problem with such a scheme is that the measurement errors resulting from decision errors may accumulate in the stored channel information, which in turn causes further decision errors. To control the error propagation, pilot blocks must be periodically inserted into the transmission to update the filter with correct channel information.

PSAM was proposed in [32]. For the STBC system with PSAM, one pilot block is inserted into the data stream every L_f blocks[32], and the estimation of the channel matrix $\boldsymbol{H}(m)$ is based on the $2L_p$ pilot blocks nearest in time to the m-th block. Thus, we define the information set

$$\begin{aligned}&\Lambda(m) = \{\boldsymbol{Y}(m')| \\ &([\![m/L_f]\!] - L_p + 1)L_f \le m' \le ([\![m/L_f]\!] + L_p)L_f\}\end{aligned} \tag{7}$$

as the set of channel measurements for the estimation of channel matrix $\boldsymbol{H}(m)$, where $[\![\cdot]\!]$ denotes the floor function. There is no error propagation in PSAM, however, decision delay is introduced, as the receiver must wait until enough pilots are received before decoding.

The estimate $\hat{\boldsymbol{H}}(m)$ of $\boldsymbol{H}(m)$ is, from [15], the conditional mean or MMSE estimate of the channel gain matrix $\boldsymbol{H}(m)$ given $\Lambda(m)$, i.e., $\hat{\boldsymbol{H}}(m) = [\hat{h}_{ij}(m)]_{M_T \times N_R} = \mathrm{E}[\boldsymbol{H}(m)|\Lambda(m)]$, and can be generated linearly from the measurements in $\Lambda(m)$. Thus, given $\Lambda(m)$, each $h_{il}(m)$ is conditionally Gaussian with mean $\hat{h}_{il}(m)$, and variance $2V^2(m)$ given by

$$2V^2(m) = \mathrm{E}[|h_{il}(m) - \hat{h}_{il}(m)|^2|\Lambda(m)] \tag{8}$$

The MSE's $2V^2(m)$ are identical for all channels due to the identical channel assumption.

D. Decoder

The optimum maximum-likelihood (ML) block-by-block receiver detects $\boldsymbol{S}(m)$ based on $\boldsymbol{R}(m)$ with the aid of the information set $\Lambda(m)$ as $\hat{\boldsymbol{S}}(m) = \arg\max_{\boldsymbol{S}(m)} p(\boldsymbol{R}(m)|\boldsymbol{S}(m), \Lambda(m))$. From (5), given $\boldsymbol{S}(m)$ and the set $\Lambda(m)$, $\boldsymbol{R}(m)$ is conditionally Gaussian with mean $\boldsymbol{S}(m)\hat{\boldsymbol{H}}(m)$. The column vectors of $\boldsymbol{R}(m)$ are independent of one another, and each has a covariance matrix of $\boldsymbol{C} = 2V^2(m)\boldsymbol{S}(m)\boldsymbol{S}^\dagger(m) + N_0\boldsymbol{I}$. Thus, the ML block-by-block receiver becomes

$$\begin{aligned}&\hat{\boldsymbol{S}}(m) = \arg\min_{\boldsymbol{S}(m)} \{N_R \ln\det(\boldsymbol{C}) + \\ &\mathrm{Tr}[(\boldsymbol{R}(m) - \boldsymbol{S}(m)\hat{\boldsymbol{H}}(m))^\dagger \boldsymbol{C}^{-1}(\boldsymbol{R}(m) - \boldsymbol{S}(m)\hat{\boldsymbol{H}}(m))]\}\end{aligned} \tag{9}$$

The detector in the form (9) makes a simultaneous decision on all the symbols of the entire block $\boldsymbol{S}(m)$. This makes the decoder computationally complex and impossible to analyze its performance in general. Thus, we consider a simpler decoder which makes independent SBS decisions. Observe that with PSK modulation, if the STBC employed satisfies:

$$\boldsymbol{S}(m)\boldsymbol{S}^\dagger(m) \propto \boldsymbol{I}_{P\times P}, \tag{10}$$

then $\boldsymbol{C}$ becomes constant and proportional to an identity matrix, and (9) simplifies to $\hat{\boldsymbol{S}}(m) = \arg\min_{\boldsymbol{S}(m)} ||(\boldsymbol{R}(m) - \boldsymbol{S}(m)\hat{\boldsymbol{H}}(m))||^2$, which can be further simplified to a SBS detector for PSK modulation where symbols carry identical energy:

$$\hat{s}_k(m) = \arg\max_{s'_k \ k'=1\ldots K} Re[z'_k(m)s'^*_k(m)] \tag{11}$$

where $z'_k(m) = \mathrm{Tr}[\boldsymbol{R}^\dagger(m)\boldsymbol{B}_{\boldsymbol{k}'}\hat{\boldsymbol{H}}(m) + \hat{\boldsymbol{H}}^\dagger(m)\boldsymbol{A}_{\boldsymbol{k}'}^\dagger\boldsymbol{R}(m)]$. This detector (11) is computationally much simpler than the detector (9). For those STBC's that satisfy condition (10), it is clear that the detector (11) is the ML block-by-block PSK detector. For such STBC's, the BEP performance analysis in Section III would give the best performance achievable. For those STBC's that do not satisfy condition (10), we continue to use the SBS detector (11), which is then a mismatched receiver. The BEP analysis results in Section III would then not represent the best performance achievable by such codes. For these latter codes, the optimum detector is the block-by-block detector in (9). A similar optimum receiver structure is also presented in [26], which shows that the gain from the optimum one is limited compared to its cost in terms of complexity.

III. Bit Error Performance Analysis

With PSK modulation, i.e., $s_k = \sqrt{E_s}e^{j\phi_k}$, the decoding rule (11) is equivalent to

$$\hat{s}_k = \arg\max_{s_k \ k=1\ldots K} Re\left\{z_k e^{-j\phi_k}\right\} \tag{12}$$

where

$$\begin{aligned} z_k =& \mathrm{Tr}[\boldsymbol{R}^\dagger \boldsymbol{B_k} \hat{\boldsymbol{H}} + \hat{\boldsymbol{H}}^\dagger \boldsymbol{A}_{\boldsymbol{k}}^\dagger \boldsymbol{R}] = x_k + u_k \\ x_k =& \sum_{k'=1}^{K} \Big\{ s_k'^{*} \mathrm{Tr}[\boldsymbol{H}^\dagger \boldsymbol{A}_k'^{\dagger} \boldsymbol{B}_k \hat{\boldsymbol{H}} + \hat{\boldsymbol{H}}^\dagger \boldsymbol{A}_k^\dagger \boldsymbol{B}_k' \boldsymbol{H}] \\ & + s_k' \mathrm{Tr}[\hat{\boldsymbol{H}}^\dagger \boldsymbol{A}_k^\dagger \boldsymbol{A}_k' \boldsymbol{H} + \boldsymbol{H}^\dagger \boldsymbol{B}_k'^{\dagger} \boldsymbol{B}_k \hat{\boldsymbol{H}}] \Big\} \\ u_k =& \mathrm{Tr}[\boldsymbol{N}^\dagger \boldsymbol{B}_k \hat{\boldsymbol{H}} + \hat{\boldsymbol{H}}^\dagger \boldsymbol{A}_k^\dagger \boldsymbol{N}] \end{aligned} \tag{13}$$

Hereafter, we drop the block index m for simplicity. For equally likely symbols, the main quantity of interest is the probability $P\left(Re[z_k e^{-j\alpha}] < 0 \mid s_k = \sqrt{E_s}\right)$ [15], where α is some angle. By conditioning on having the information set Λ, we first evaluate the conditional probability $P\left(Re[z_k e^{-j\alpha}] < 0 \mid s_k = \sqrt{E_s}, \Lambda\right)$. Since Λ is a set of Gaussian r.v.'s, it follows that x_k in (13) is a conditionally complex Gaussian r.v. given s_k and Λ, with mean $s_k \sum_{i=1}^{M_T} \sum_{l=1}^{N_R} \lambda_{i,k} |\hat{h}_{il}|^2$ and variance $2V^2 E_s \sum_{i=1}^{M_T} \sum_{l=1}^{N_R} \omega_{i,k} |\hat{h}_{il}|^2$, where $\{\omega_{i,k}\}_{i=1}^{M_T}$ are positive numbers given by

$$\omega_{i,k} = \sum_{k'=1}^{K} \sum_{j=1}^{M_T} \left[|\boldsymbol{a}_k'^{j\dagger} \boldsymbol{b}_k^i|^2 + |\boldsymbol{b}_k'^{j\dagger} \boldsymbol{b}_k^i|^2 + |\boldsymbol{a}_k^{i\dagger} \boldsymbol{b}_k'^{j}|^2 + |\boldsymbol{a}_k^{i\dagger} \boldsymbol{a}_k'^{j}|^2 \right] \tag{14}$$

and where $\{\boldsymbol{a}_k^i, \boldsymbol{b}_k^i\}_{i=1}^{M_T}$ are $P \times 1$ column vectors of $\boldsymbol{A}_k, \boldsymbol{B}_k$. The definition of $\omega_{i,k}$ in (14) can be obtained from the properties of orthogonal STBC's in (2) and (3), by re-writing the matrices in terms of their column vectors. Similarly, in (13) the quantity u_k is also a complex Gaussian r.v. conditioning on Λ, with mean zero and variance $N_0 \sum_{i=1}^{M_T} \sum_{l=1}^{N_R} \lambda_{i,k} |\hat{h}_{il}|^2$. From (13), it is straightforward to show that z_k is conditionally a complex Gaussian r.v. given by

$$\begin{aligned} (z_k | s_k, \Lambda) \sim N \Bigg(& s_k \sum_{i=1}^{M_T} \sum_{l=1}^{N_R} \lambda_{i,k} |\hat{h}_{il}|^2 , \\ & E_s 2V^2 \sum_{i=1}^{M_T} \sum_{l=1}^{N_R} \omega_{i,k} |\hat{h}_{il}|^2 + N_0 \sum_{i=1}^{M_T} \sum_{l=1}^{N_R} \lambda_{i,k} |\hat{h}_{il}|^2 \Bigg) \end{aligned} \tag{15}$$

Thus, the quantity $Re\left\{z_k e^{-j\alpha}\right\}$ in (12) is conditionally a Gaussian variable with variance $E_s V^2 \sum_{i=1}^{M_T} \sum_{l=1}^{N_R} \omega_{i,k} |\hat{h}_{il}|^2 + \frac{N_0}{2} \sum_{i=1}^{M_T} \sum_{l=1}^{N_R} \lambda_{i,k} |\hat{h}_{il}|^2$ and mean $\sqrt{E_s} \cos(\phi_k - \alpha) \sum_{i=1}^{M_T} \sum_{l=1}^{N_R} \lambda_{i,k} |\hat{h}_{il}|^2$. The conditional probability $P_{e|\Lambda} = P(Re\left\{z_k e^{-j\alpha}\right\} < 0 | s_k, \Lambda)$ can now be evaluated as

$$P_{e|\Lambda} = Q\left(\sqrt{ \frac{ E_s \cos^2(\phi_k - \alpha) \left(\sum\limits_{i=1}^{M_T} \sum\limits_{l=1}^{N_R} \lambda_{i,k} |\hat{h}_{il}|^2 \right)^2 }{ E_s V^2 \sum\limits_{i=1}^{M_T} \sum\limits_{l=1}^{N_R} \omega_{i,k} |\hat{h}_{il}|^2 + \frac{N_0}{2} \sum\limits_{i=1}^{M_T} \sum\limits_{l=1}^{N_R} \lambda_{i,k} |\hat{h}_{il}|^2 } } \right) \tag{16}$$

Next, we have to average over the estimates $\hat{h}_{il}(m)$ in (16) to obtain the average error probability $P(Re\left\{z_k e^{-j\alpha}\right\} < 0 | s_k = \sqrt{E_s})$. Defining

$$\begin{aligned} \rho_{i,k} &= \omega_{i,k} / \lambda_{i,k}, \\ \rho_{\max,k} &= \max_{i=1\ldots M_T} \{\rho_{i,k}\}, \rho_{\min,k} = \min_{i=1\ldots M_T} \{\rho_{i,k}\}, \\ \lambda_{\max,k} &= \max_{i=1\ldots M_T} \{\lambda_{i,k}\}, \lambda_{\min,k} = \min_{i=1\ldots M_T} \{\lambda_{i,k}\}, \end{aligned} \tag{17}$$

the probability in (16) can be bounded as

$$\begin{aligned} & Q\left(\sqrt{ \frac{ \lambda_{\max,k} E_s \cos^2 \alpha \sum_{i=1}^{M_T} \sum_{l=1}^{N_R} |\hat{h}_{il}|^2 }{ \rho_{\min,k} E_s V^2 + \frac{N_0}{2} } } \right) \le P_{e|\Lambda} \\ & \le Q\left(\sqrt{ \frac{ \lambda_{\min,k} E_s \cos^2 \alpha \sum_{i=1}^{M_T} \sum_{l=1}^{N_R} |\hat{h}_{il}|^2 }{ \rho_{\max,k} E_s V^2 + \frac{N_0}{2} } } \right) \end{aligned} \tag{18}$$

The equality signs hold in (18) when

$$\lambda_{i,k} = \lambda_k, \ \omega_{i,k} = \omega_k, \ \text{for all } i = 1 \ldots M_T, \tag{19}$$

and the $\rho_{i,k}$'s will then have a common value $\rho_k = \omega_k / \lambda_k$, for all $i = 1 \ldots M_T$. Since the estimates $\hat{h}_{il}(m)$'s are themselves complex Gaussian r.v.'s, each with mean zero and variance $2[\Omega(0) - V^2(m)]$ [15], [27]. Therefore, the quantity $d^2(m) = \sum_{i=1}^{M_T} \sum_{l=1}^{N_R} |\hat{h}_{il}(m)|^2$ in (18) has a chi-square pdf with $2M_T N_R$ degrees of freedom [30](eq. 2-1-110). Using this pdf to average the upper and lower bounds in (18) over the quantity $d^2(m)$ gives the result [30](Sect. 14.4)

$$\begin{aligned} F(\alpha, \mu(\rho_{\min,k}, \lambda_{\max,k})) \le P(Re\left\{z_k e^{-j\alpha}\right\} < 0 | s_k = \sqrt{E_s}) \\ \le F(\alpha, \mu(\rho_{\max,k}, \lambda_{\min,k})) \end{aligned} \tag{20}$$

Here, the function $F(\alpha, \mu)$ is given by

$$\begin{aligned} F(\alpha, \mu) = & \left[\frac{1-\mu}{2} \right]^{M_T N_R} \\ & \cdot \sum_{k=0}^{M_T N_R - 1} \begin{pmatrix} M_T N_R - 1 + k \\ k \end{pmatrix} \left[\frac{1+\mu}{2} \right]^k \end{aligned} \tag{21}$$

where

$$\begin{aligned} \mu(\rho, \lambda) &= \left(1 + \frac{N_R + \rho \gamma_s (1-\eta)}{\lambda \gamma_s \eta \cos^2 \alpha} \right)^{-1/2}, \\ \gamma_s &= N_R \frac{2\Omega(0) E_s}{N_0}, \quad \text{and} \quad \eta = 1 - \frac{V^2(m)}{\Omega(0)} \end{aligned} \tag{22}$$

The bounds in (20) describe the error performance of a single signal symbol s_k. As there are K symbols in one block, the average BEP is obtained from the average probability $\Gamma(\alpha)$ given by

$$\Gamma(\alpha) = \tfrac{1}{K} \textstyle\sum_{k=1}^{K} P(Re\left\{z_k e^{-j\alpha}\right\} < 0 | s_k = \sqrt{E_s}) \tag{23}$$

Now, for Gray coded PSK, it is clear that the BEP is given by [28]

$$\begin{aligned} P_b^{BPSK} = \Gamma(0) \quad , \quad P_b^{QPSK} = \Gamma(\pi/4), \\ P_b^{8PSK} \approx \tfrac{2}{3} \Gamma(3\pi/8)[1 + \Gamma(\pi/8)] \end{aligned} \tag{24}$$

In addition to these two tight upper and lower bounds in (20), $\Gamma(\alpha)$ also admits a Chernoff upper bound by applying the bound $Q(x) < 0.5 e^{-x^2/2}$ to the upper bound in (18):

$$\Gamma(\alpha) < \frac{1}{2K} \sum_{k=1}^{K} \left(1 + \frac{\lambda_{\min,k} \gamma_s \eta \cos^2 \alpha}{N_R + \rho_{\max,k} \gamma_s (1-\eta)} \right)^{-M_T N_R} \tag{25}$$

The Chernoff bound in (25) shows clearly that the BEP decays exponentially with the product $M_T N_R$ of the number of transmit and receive antennas.

TABLE I
PARAMETERS LIST FOR BEP EVALUATION

	STBC proposed in	Size ($P \times M_T$)	Rate	$[\lambda_{\min,k}; \rho_{\max,k}]$ upper bound	$[\lambda_{\max,k}; \rho_{\min,k}]$ lower bound
STBC with exact BEP evaluation	[5] (Real Orthogonal Designs)	2×2	1	[1; 2]	
		$4 \times 4, 3$	1	[1; 4,3]	
		$8 \times 8, 7, 6, 5$	1	[1; 8, 7, 6, 5]	
	[15] (1Tx case)	1×1	1	[1; 1]	
	[4] (Alamouti)	2×2	1	[1; 2]	
	[5], [6]	4×4	3/4	[1; 3]	$[\lambda_{\max,k}; \rho_{\min,k}] = [\lambda_{\min,k}; \rho_{\max,k}]$
	[13]	30×6	2/3	[1; 4]	
	[14]	56×8	5/8	[1; 5]	
	[5] (Systematically Constructed Half-Rate STBC's)	4×2	1/2	[2; 2]	
		$8 \times 4, 3$		[2; 4, 3]	
		$16 \times 8, 7, 6, 5$		[2; 8, 7, 6, 5]	
STBC with lower/upper bound for BEP evaluation	[5], [6]	4×3	3/4	[1; 3]	[1; 2]
	[8]	7×4	4/7	[1; 4]	[1; 2]
	[8]	11×5	5/8	[1; 4]	$[2;3]_{k=1,2,3}$ $[1;3]_{k=4,5,6,7}$
	[9], [10]	15×5	2/3	[1; 4]	[1; 3]
	[8]	30×6	$3/5$	$[1;5]_{k=1\ldots11,18}$ $[1;4]_{k=12\ldots17}$	$[2;4]_{k=1,2,3}[2;3.5]_{k=4\ldots11}$ $[1;4]_{k=12\ldots17}[1;3]_{k=18}$
	[12]	56×7	5/8	[1; 5]	[1; 4]

When condition (19) is satisfied, the upper and lower bounds in (18) and hence those in (20) coincide with each other. The BEP expression in (23) is now given by

$$\Gamma(\alpha) = \frac{1}{K} \sum_{k=1}^{K} F(\alpha, \mu(\rho_k, \lambda_k)) \tag{26}$$

A summary of those known STBC's having the exact BEP expression (26) is given in the upper half of Table I. For those special square designs satisfying $\boldsymbol{S}^\dagger \boldsymbol{S} = \boldsymbol{S}\boldsymbol{S}^\dagger = \boldsymbol{I} \cdot \sum_{k=1}^{K} |s_k|^2$ in Table I, it can be shown from (14) that $\omega_{i,k} = K, \rho_k = K, \lambda_k = 1,$ for all k when calculating (26).

When condition (19) cannot be met, it is impossible to average (16) over all channel estimates analytically. Only the bounds in (18) can be obtained in general. It will be shown in Section V that these two bounds still provide very good approximations to the BEP performance. Those orthogonal STBC's that do not satisfy (19) are illustrated in the lower half of Table I.

IV. FADING MODELS, CHANNEL ESTIMATION, AND THEORETICAL BEP COMPUTATION

We illustrate the BEP computation using Markov channel models with DF, KF channel estimation, and Jakes' model with DF and PSAM Wiener filter (WF) channel estimation.

A. Channel Models

1) A.1 Markov Channel Models: Here, the in-phase component $a_{i,l}(m) = Re[h_{i,l}(m)]$ and the quadrature-phase component $b_{i,l}(m) = Im[h_{i,l}(m)]$ of each fading process evolve according to a model

$$\boldsymbol{x}_{i,l}(m+1) = \boldsymbol{F}\, \boldsymbol{x}_{i,l}(m) + \boldsymbol{G}\, \boldsymbol{w}_{i,l}(m) \tag{27}$$

of appropriate dimension, and where $\{\boldsymbol{w}_{i,l}(m)\}_{m=0}^{\infty}$ is a sequence of input AWGN with $\mathrm{E}[\boldsymbol{w}_{i,l}(m)] = \boldsymbol{0}$ and $\mathrm{E}[\boldsymbol{w}_{i,l}(m)\boldsymbol{w}_{i,l}^T(m')] = \boldsymbol{Q}\delta_{mm'}$. We consider here in particular the case of a first-order Butterworth (1BTW) and a third-order Butterworth (3BTW) model for the channel.

In the 1BTW model, we have $F = \exp[-\omega_d T]$, G = 1, and $Q = \sigma^2(1 - e^{-2\omega_d T})$. T is the interval between discrete time points. In the 3BTW model, we have

$$\boldsymbol{x}_{i,l}(m) = \begin{pmatrix} x_{i,l}^{(1)}(m) \\ x_{i,l}^{(2)}(m) \\ x_{i,l}^{(3)}(m) \end{pmatrix}, \boldsymbol{G} = \begin{pmatrix} 0 \\ 0 \\ 1 \end{pmatrix}, Q = 3\sigma^2\, \omega_d T,$$
$$\boldsymbol{F} = \begin{pmatrix} 1 & \omega_d T & 0 \\ 0 & 1 & \omega_d T \\ -\omega_d T & -2\omega_d T & 1 - 2\omega_d T \end{pmatrix}. \tag{28}$$

2) Jakes' Model: In Jakes' model [31], the correlation function is given by

$$2\Omega(m) = \mathrm{E}[h_{i,l}(n)h_{i,l}^*(n-m)] = 2\sigma^2\, J_0(m\omega_d T) \tag{29}$$

where $J_0(\cdot)$ is the zero-th order Bessel function of the first kind.

B. Channel Estimation

When a state-space channel model is available, the KF is the optimum channel estimator. The KF is more suitable for the DF channel estimation scheme since it can operate recursively in time as symbol decisions are made. Given the measurements $\boldsymbol{\Lambda}(m) = \{\boldsymbol{Y}(m')\}_{m'=0}^{m-1}$ and the model (27), it is easy to follow [29] and write down the KF for generating the estimates $\hat{\boldsymbol{H}}(m) = \mathrm{E}\left[\boldsymbol{H}(m)\,|\boldsymbol{\Lambda}(m)\right]$, for the Butterworth models. A block-wise constant channel assumption is adopted by setting $T = T_B$ in (27) and using the equivalent fade rate $\omega_d T_B$ for the theoretical computation, where $T_B = PT_s$ is the block duration, and T_s is the symbol period. $V^2(m)$ can be obtained by solving the Riccati equations in [29]. $V^2(m)$ is recursively computed until a steady state value V_∞^2 is reached, V_∞^2 which is then used for BEP computation.

For Jakes' channel model, a WF with L_w taps [27] is used, and the estimate is given by $\hat{h}_{i,l}(m) = \boldsymbol{w}_i^T \tilde{\boldsymbol{y}}_{il}(m)$, where $\tilde{\boldsymbol{y}}_{il}(m) = [y_{il}(m-1), \ldots, y_{il}(m-L_w)]^T$, $\boldsymbol{\Xi}_i =$

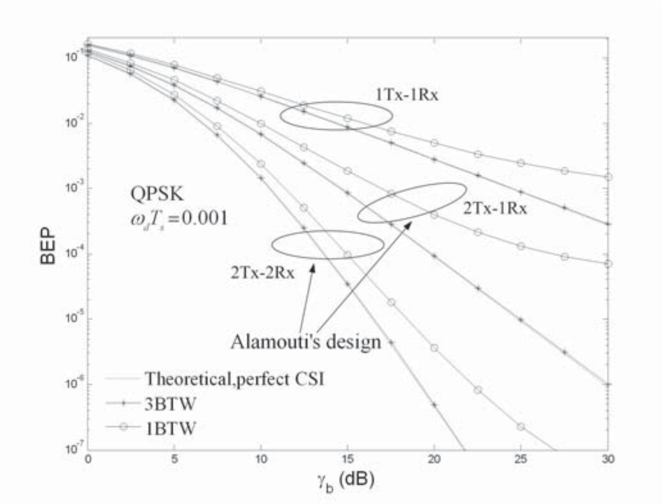

Fig. 2. Theoretical BEP performance of QPSK under Butterworth channel models using KF estimator (2Tx-1Rx = 2 transmit and 1 receive antenna).

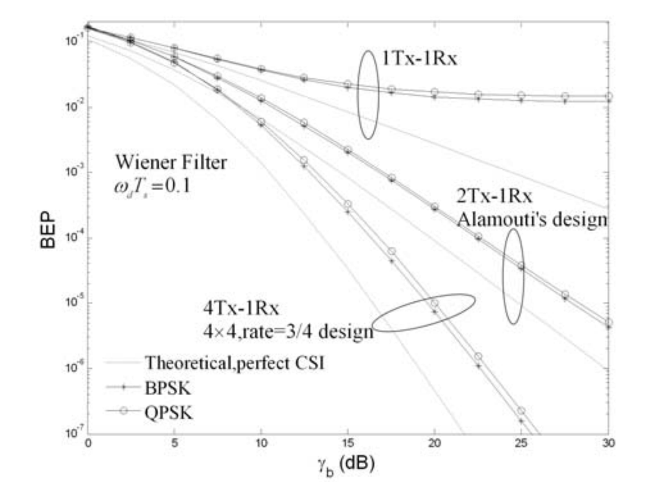

Fig. 3. Theoretical BEP performance comparison with different numbers of transmit antennas under Jakes' channel model using DF WF estimator.

$\mathrm{E}[\tilde{\boldsymbol{y}}_{il}(m)\tilde{\boldsymbol{y}}_{il}^{\dagger}(m)]$ $\boldsymbol{p}_i = \mathrm{E}[h_{il}(m)\tilde{\boldsymbol{y}}_{il}^{\dagger}(m)]$ and $\boldsymbol{w}_i = \boldsymbol{\Xi}_i^{-1}\boldsymbol{p}_i$. The MSE of the filter is

$$V^2(m) = \Omega(0) - \boldsymbol{p}_i^T \boldsymbol{w}_i \tag{30}$$

where $\Omega(m)$ is defined in (29) with $T = T_B$. Similarly, for a PSAM system, one can only use a Wiener filter channel estimator where the estimation is based on the nearest $2L_p$ pilot blocks. The MSE of a PSAM system can also be calculated by (30), using the set $\Lambda(m)$ given in (7).

V. Theoretical Performance and Simulation Results

In the simulations, 10 preamble blocks are first sent to enable the KF to acquire the channel estimates accurately before data detection, and one pilot block is periodically inserted into the transmission after every 9 data blocks. For Jakes' channel model, a decision-feedback WF with 10 taps is used, and in the PSAM scheme the estimator uses the 10 nearest pilot blocks for generating the estimates. Using the above results, the BEP's of MPSK are computed and plotted against the total mean received SNR per bit given by $\gamma_b = (10\ /\ 9)\gamma_s \sum_{i=1}^{M_T}\sum_{k=1}^{K}\lambda_{i,k}/K\log_2 M$, where the factor (10 / 9) accounts for the energy in the pilot symbols. These BEP results represent the actual performance achievable by our receiver, under a block-wise constant channel model. BEP performances of Alamouti's scheme with Butterworth channel models are demonstrated in Fig. 2. Also plotted are the BEP with perfect CSI at the receiver with $V^2(m) = 0$, as well as the conventional one-transmit antenna result obtained from [15] to show the diversity gains. As mentioned in Section IV, the performance calculation is based on the assumption of block-wise constant channel and, thus, uses the block normalized fade rate $\omega_d T_B$ instead of $\omega_d T_s$. This idea is used throughout this section unless otherwise stated. For a low fade rate $\omega_d T_B = 0.001$, the performance under the 3BTW channel is almost the same as that of the receiver with perfect CSI. However, performance under the 1BTW channel is worse than that under the 3BTW channel. This is because for the same fade rate, the 3BTW channel fluctuates more slowly than the 1BTW channel does. We use Alamouti's design [4] and the 4×4 rate-3/4 designs in [5], [6] in Fig. 3, and as it shows, for a faster channel with a normalized fade rate of $\omega_d T_s = 0.1$, the performance curves with channel estimation deviate more from those with perfect CSI, with the deviation being greater for the QPSK than for the BPSK modulation. In Fig. 4, we compare the performances of the 2×2, 4×4, and 8×8 full-rate real designs with, respectively, the systematically constructed 4×2, 8×4, and 16×8 half-rate COD proposed in [5], respectively. The half-rate codes use QPSK, for fair comparison. According to Table I, they have identical performances when CSI is perfectly known. Under a 1BTW channel of $\omega_d T_s = 0.001$, it is shown that the full-rate designs with shorter block length P outperform their corresponding half-rate ones, and the performance gap between them becomes larger as P increases. This loss is only due to the increased block fade rate $\omega_d T_B$. One can expect more loss due to a longer block length P when the channel fluctuates even faster. This indicates that in designing a practical STBC, one should keep the block length P small while gaining from the space-time diversity. When P is too large, the resulting performance loss due to channel fluctuations might be greater than the diversity gain, resulting in a worse overall performance.

The BEP curve of our receiver asymptotically reaches an irreducible floor as the SNR approaches infinity. As for any nonzero channel fade rate $\omega_d T_s$, $\hat{\boldsymbol{H}}(m)$ is a predicted estimate with an irreducible, nonzero error variance, which leads to the error floor.

As discussed in Section IV, an exact BEP expression cannot be obtained for those STBC's not satisfying condition (19). In Fig. 2, the upper bound and lower bound of several such STBC's in Table I are plotted. It can be seen that with $\omega_d T_s = 0.005$ and PSAM, these two bounds are very close to each other, and thus provide a very good approximation to the actual BEP.

Since the results so far were obtained under the assumption that the channel is constant over a block, it would be of interest to know how accurately our theoretical BEP results predict the actual performance under a channel fluctuating from one

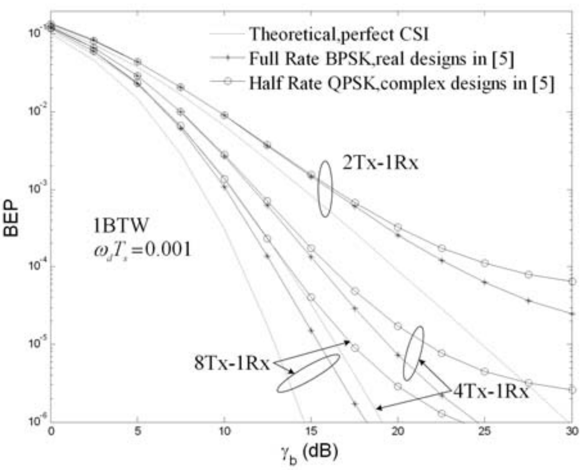

Fig. 4. Theoretical BEP performance comparison between full- and half-rate STBC's under Jakes' channel model using PSAM.

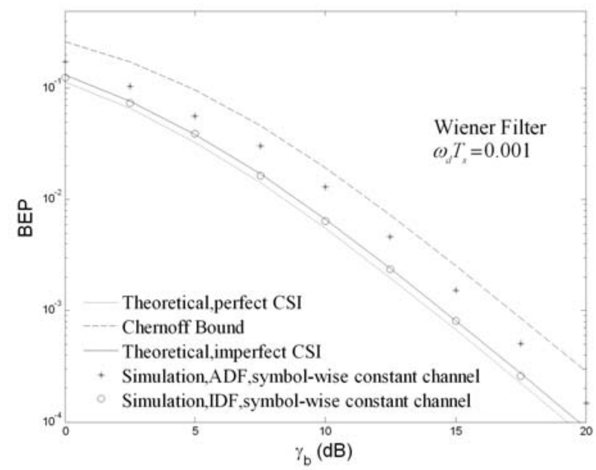

Fig. 6. BEP of BPSK with Alamouti's STBC with one receive antenna under Jakes' channel model.

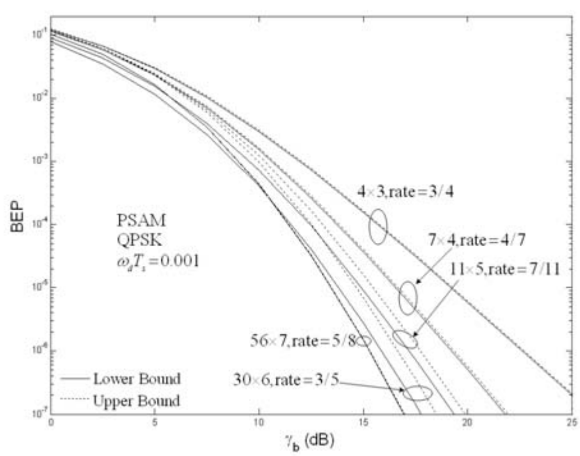

Fig. 5. Theoretical bounds of BEP performance for different STBC under Jakes' channel model using PSAM.

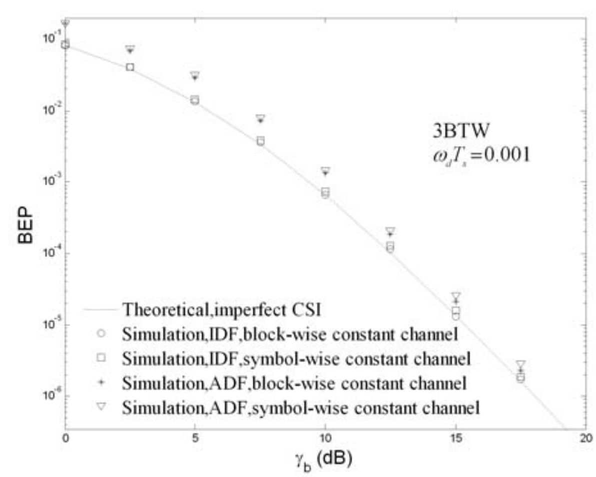

Fig. 7. BEP Performance of rate-3/4 STBC with QPSK under 3BTW channel.

symbol period to the next. Fig. 6 shows the BPSK performance under Jakes' fading channel with Alamouti's scheme for a single receive antenna. The simulation is conducted under a symbol-wise constant channel while the theoretical BEP performances were obtained under the block-wise constant assumption. It can be seen in Fig. 6 that the simulation result is close to the theoretical performance, with an around-1dB gap. To show the cause of this performance gap, we simulated the case with ideal decision feedback (IDF). In contrast to the actual decision feedback (ADF) mode, the IDF estimator uses $\boldsymbol{S}(m)$ instead of $\hat{\boldsymbol{S}}(m)$ when computing (6), so that erroneous decision-feedbacks are removed. The IDF simulation result matches perfectly the theoretical calculation with imperfect CSI, which means the gap between ADF and theoretical performance is almost completely caused by error propagation; and a realistic channel with $\omega_d T_s = 0.001$ is slow enough to validate the block-wise constant assumption. It is sound to make such an assumption in our derivations.

In Fig. 7, we adopt the 4×4 rate-3/4 STBC proposed in [6] under a 3BTW channel. Besides the IDF condition, we also generate a block-wise constant channel for simulation. The curves in the figure clearly show the factors that influence the STBC performance. The simulation results with block-wise constant channel and IDF match the theoretical prediction perfectly, thus validating our analysis. The performance difference between the symbol-wise constant channel case and the block-wise constant channel case is due to the channel fluctuations within the block in the symbol-wise constant channel that disturb the orthogonality of the STBC. Similar to Fig. 6, the error propagation is still the main reason for the performance degradation in an actual STBC system. We use PSAM in Fig. 8 to remedy this problem. The simulation is carried out under a fast fading Jakes' channel with $\omega_d T_B = 0.2$. Again, the simulation under a block-wise constant channel matches the theoretical performance perfectly, and the loss caused by the symbol-to-symbol fluctuation of the channel is within 1dB even under high SNR. PSAM is thus preferable to a DF system for channel estimation when the STBC block length is not very large.

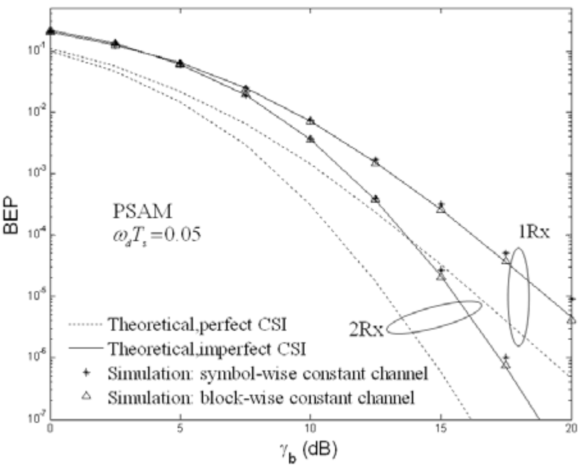

Fig. 8. BEP performance of rate-3/4 STBC with QPSK under Jakes' channel model using PSAM.

VI. Conclusions

We presented a SBS channel estimation receiver for space-time block coded systems. A simple, closed-form expression for its BEP is obtained, showing clearly the dependence of the BEP on the channel estimation MSE. We simulated the receiver under the more realistic assumption that the channel is constant over only a symbol period, and fluctuates from one symbol period to the next. The simulations validate the theoretical performance prediction, and verify that the accuracy of the latter prediction depends on the fade rate $\omega_d T_s$.

References

[1] E. Telatar, "Capacity of multi-antenna Gaussian channels," AT&T Bell Labs Internal Technical Memo, 1995.

[2] G. J. Foschini, Jr. and M. J. Gans, "On limits of wireless communication in a fading environment when using multiple antennas," *Wireless Personal Commun.*, Mar. 1998.

[3] V. Tarokh, N. Seshadri, and A. R. Calderbank, "Space-time codes for high data rate wireless communication: performance criterion and code construction," *IEEE Trans. Inform. Theory*, vol. 44, pp. 744-765, Mar. 1998.

[4] S. M. Alamouti, "A simple transmitter diversity scheme for wireless communications," *IEEE J. Select. Areas Commun.*, vol. 16, pp. 1451-1458, Oct. 1998.

[5] V. Tarokh, H. Jafarkhani, and A. R. Calderbank, "Space-time block codes from orthogonal design," *IEEE Trans. Inform. Theory*, vol. 45, pp. 1456-1467, July 1999.

[6] G. Ganesan and P. Stioca, "Space-time block codes: a maximum SNR approach," *IEEE Trans. Inform. Theory*, pp. 1650-1656, Apr. 2001.

[7] O. Tirkkonen and A. Hottinen, "Square-matrix embeddable space-time block codes for complex signal constellations," *IEEE Trans. Inform. Theory*, vol. 48, pp. 1122-1126, Feb. 2002

[8] W. Su and X. -G. Xia "Two generalized complex orthogonal space-time block codes for rates 7/11 and 3/5 for 5 and 6 transmit antennas," *IEEE Trans. Inform. Theory*, vol. 49, pp. 313-316, Jan. 2003.

[9] X. -B. Liang, "A high-rate orthogonal space-time block code," *IEEE Commun. Lett.*, vol. 7, pp. 222-223, May 2003.

[10] C. Xu, Y. Gong, and K. B. Letaief, "High-rate complex orthogonal space-time block codes for high number of transmit antennas," in *Proc. IEEE ICC' 2004*, vol. 2, pp. 20-24, June 2004.

[11] H. Wang and X.-G. Xia, "Upper bounds of rates of space-time block codes from complex orthogonal designs," *IEEE Trans. Inform. Theory*, vol. 49, pp. 2788-2796, Oct. 2003.

[12] X.-B. Liang, "Orthogonal designs with maximal rates," *IEEE Trans. Inform. Theory*, vol. 49, no. 10, pp. 2468-2503, Oct. 2003.

[13] W. Su, X.-G Xia, and K. J. Ray Liu, "A systematic design of high-rate complex orthogonal space-time block codes," *IEEE Commun. Lett.*, vol. 8, pp. 380-382, June 2004.

[14] K. Lu, S. Fu, and X.-G Xia, "Closed-form designs of complex orthogonal space-time block codes of rates (k+1)/(2k) for 2k-1 or 2k transmit antennas," *IEEE Trans. Inform. Theory*, vol. 51, no. 12, pp. 4340-4347, Dec. 2005.

[15] P. Y. Kam, "Optimal detection of digital data over the nonselective Rayleigh fading channel with diversity reception," *IEEE Trans. Commun.*, vol. 39, pp. 214-219, Feb. 1991.

[16] C. Gao, A. Haimovich, and D. Lao, "Bit error probability for space-time block code with coherent and differential detection," in *Proc. VTC2002 Fall*, Sept., 2002.

[17] H. Zhang and T. A. Gulliver, "Capacity and error probability analysis for orthogonal space-time block codes over fading channels," *IEEE Trans. Wireless Commun.*, vol. 4, pp. 808-819, Mar. 2005.

[18] L. Xian and H. Liu, "Exact error probability for space-time block-coded MIMO systems over Rayleigh fading channels," *IEE Proc. Commun.*, vol. 152, pp. 197-201, Apr. 2005.

[19] J. Yuan, "On the performance of space-time block codes on slow rayleigh fading channels," in *Proc. IEEE PIMRC' 2003*, vol. 2, pp. 1688-1692, Sept. 2003.

[20] H. Shin and J. H. Lee, "Performance analysis of space-time block codes over keyhole Nakagami-m fading channels," *IEEE Trans. Veh. Technol.*, vol. 53, no. 2, Mar. 2004.

[21] G. R. Mohammad-Khani, V. Meghdadi, J. P. Cances, and L. Azizi, "Maximum likelihood decoding rules for STBC generalized framework for detection and derivation of accurate upperbounds," in *Proc. ICC 2004*, vol. 5, pp. 2578-2583, June 2004.

[22] P. Garg, R. K. Mallik, and H. A. Gupta, "Performance analysis of space-time coding with imperfect channel estimation," in *Proc. IEEE International Conference on Personal Wireless Communications*, pp. 71-75, Dec. 2002.

[23] H. Cheon and D. Hong, "Performance analysis of space-time block codes in time-varying Rayleigh fading channels," in *Proc. IEEE ICASSP' 2002*, vol. 3, pp, 2357-2360, May 2002.

[24] C. Cozzo and B. L. Hughes, "An adaptive receiver for space-time trellis codes based on per-survivor processing," *IEEE Trans. Commun.*, vol. 50, pp. 1213-1216, Aug. 2002

[25] Z. Liu, X. Ma, and G. B. Giannakis, "Space-time coding and Kalman filtering for time-selective fading channels," *IEEE Trans. Commun.*, vol. 50, pp. 183-186, Feb. 2002.

[26] G. Tarrico and E. Biglieri, "Decoding space-time coding with imperfect channel estimation," in *Proc. International Conference on Communications (ICC' 2004)*, June, 2004

[27] P. Y. Kam and C. H. Teh, "Reception of PSK signals over fading channels via quadrature amplitude estimation," *IEEE Trans. Commun.*, vol. 31, pp. 1024-1027, Aug. 1983.

[28] P. J. Lee, "Computation of the bit error rate of coherent M-ary PSK with Gray code bit mapping," *IEEE Trans. Commun.*, vol. COM-34, pp. 488-491, May 1986.

[29] B. Anderson and J. B. Moore, *Optimal Filtering*. Englewood Cliffs, NJ: Prentice-Hall, 1979.

[30] J. G. Proakis, *Digital Communication*, 4th Edition. McGraw-Hill, 2000.

[31] W. C. Jakes, ed., *Microwave Mobile Communications*. New York: Wiley, 1974.

[32] J. K. Cavers, "An analysis of pilot symbol assisted modulation for Rayleigh fading channel," *IEEE Trans. Veh. Technol.*, vol. 40, no. 4, pp. 686-693, Nov. 1991.

Cheng Shan received the B.Eng. and M.Eng. degrees in electrical engineering from Zhejiang University, Hangzhou, China, in 1998 and 2001, respectively. He received the Ph.D degree in electrical engineering from National University of Singapore in 2006.

From 2005, he has been with the Global Standard Research Team, Telecommunication&Network R&D Center, Samsung Electronics Co. Ltd., in Suwon, South Korea. His research interests include: MIMO signal processing and implementations, cognitive radio techniques, and wireless communication standardization.

Pooi Yuen Kam [M '83, SM'87] was born in Ipoh, Malaysia in 1951, and educated at the Massachusetts Institute of Technology, Cambridge, Mass., where he obtained the S. B., S. M., and Ph. D. degrees in electrical engineering in 1972, 1973, and 1976, respectively.

From 1976 to 1978, he was a member of the technical staff at the Bell Telephone Laboratories, Holmdel, N. J., where he was engaged in packet network studies. Since 1978, he has been with the Department of Electrical and Computer Engineering, National University of Singapore, where he is now a professor. He served as the Deputy Dean of Engineering and the Vice Dean for Academic Affairs, Faculty of Engineering of the National University of Singapore, from 2000 to 2003. His research interests are in detection and estimation theory, digital communications and coding. He spent the sabbatical year 1987 to 1988 at the Tokyo Institute of Technology, Tokyo, Japan, under the sponsorship of the Hitachi Scholarship Foundation. In year 2006, he was invited to the School of Engineering Science, Simon Fraser University, Burnaby, B.C., Canada as the David Bested Fellow.

Dr. Kam is a member of Eta Kappa Nu, Tau Beta Pi, and Sigma Xi. Since 1996, he has been the Editor for Modulation and Detection for Wireless Systems of the IEEE TRANSACTIONS ON COMMUNICATIONS. He won the Best Paper Award at the IEEE VTC 2004 - Fall.

Arumugam Nallanathan (S'97−M'00−SM'05) received the B.Sc. with honors from the University of Peradeniya, Sri-Lanka, in 1991, the CPGS from the Cambridge University, United Kingdom, in 1994 and the Ph.D. from the University of Hong Kong, Hong Kong, in 2000, all in Electrical Engineering. He was an Assistant Professor in the Department of Electrical and Computer Engineering, National University of Singapore, Singapore from August 2000 to December 2007. Currently, he is a Senior Lecturer in the Department of Electronic Engineering at King's College London, United Kingdom. His research interests include OFDM systems, ultra-wide bandwidth (UWB) communication and localization, MIMO systems, and cooperative diversity techniques. In these areas, he has published over 120 journal and conference papers. He is a co-recipient of the Best Paper Award presented at 2007 IEEE International Conference on Ultra-Wideband (ICUWB'2007).

He currently serves on the Editorial Board of IEEE TRANSACTIONS ON WIRELESS COMMUNICATIONS, IEEE TRANSACTIONS ON VEHICULAR TECHNOLOGY, John Wiley's WIRELESS COMMUNICATIONS AND MOBILE COMPUTING and EURASIP JOURNAL OF WIRELESS COMMUNICATIONS AND NETWORKING as an Associate Editor. He served as a Guest Editor for EURASIP JOURNAL OF WIRELESS COMMUNICATIONS AND NETWORKING: Special issue on UWB Communication Systems- Technology and Applications. He also served as a technical program committee member for more than 25 IEEE international conferences. He currently serves as the General Track Chair for IEEE VTC'2008-Spring, Co-Chair for the IEEE GLOBECOM'2008 Signal Processing for Communications Symposium, and IEEE ICC'2009 Wireless Communications Symposium.